First-principles study of anatase and rutile TiO_2 doped with Eu ions: A comparison of GGA and LDA+U calculations

A. Rubio-Ponce
Departamento de Ciencias Básicas, Universidad Autónoma Metropolitana-Azcapotzalco, Av. San Pablo 180, C.P. 02200, México, Distrito Federal, Mexico

A. Conde-Gallardo and D. Olguín
Departamento de Física, Centro de Investigación y de Estudios Avanzados del Instituto Politécnico Nacional, A.P. 14740, C.P. 07300, México, Distrito Federal, Mexico

(Received 27 June 2007; revised manuscript received 18 March 2008; published 9 July 2008)

Here, we study some changes on the electronic band structure of anatase and rutile TiO_2 doped with Eu ions using first-principles calculations. This work presents a comparison of a GGA and LDA+U calculations. It was found that the GGA calculations show better agreement with experimental data than LDA+U calculations. From our study a series of highly localized states in the host matrix band gap was found. According to our calculations, and as it is widely known, these states are mainly Eu $4f$ character. However, contrary to the common idea that Eu orbitals should be localized as atom-free-like states, our calculations show that Eu orbitals hybridize with the host oxygen and titanium orbitals; the same occurs in the valence band, as well as in the conduction band region.

DOI: 10.1103/PhysRevB.78.035107 PACS number(s): 71.15.Mb, 71.20.Eh

I. INTRODUCTION

Recently, experimental work have renewed interest in the wide band-gap transition-metal oxide semiconductors because it seems that when they are doped with appropriate ions, these materials develop some unexpected physical properties, which could have important consequences in developing technology. For example, recently it has been shown that titanium dioxide (TiO_2) or zinc oxide (ZnO) (Refs. 1 and 2) doped with magnetic ions, cobalt or manganese, magnetic ordering can be induced in these hosting materials. In the same way, experimental groups have shown that when TiO_2 is doped with rare earth (RE) ions, important luminescent effects can be observed in these compounds.[3–13]

Therefore, characterization of these solid state materials is being a matter of study by different groups. However, so far, most of the work has been addressed from experimental point of view, and nothing has been done from solid state physics first principles. Indeed, the problem of electronic band structure and electronic density of states of pure metal oxides have been studied by several groups in the past; the problem of different impurities effects in these wide band-gap semiconductors has not been addressed. So, in the present work a theoretical study of the effect on the electronic band structure of TiO_2 doped with RE ions was done. Experimentally it has been shown that TiO_2:RE materials present sharp, near-monochromatic luminescent lines, in similar positions to those observed in other host matrices doped with similar ions. Because of that, there is agreement in associating the emission to the electronic structure of RE ions. However, the width and relative intensity of the lines frequently depend on the crystal symmetry of the matrix. Thus, depending on the host material, some lines are present while others are inactive. This feature can be used to tune the material for specific applications.[4–6]

On the other hand, although it is widely accepted that the RE f-f transitions are almost independent of the host matrix,[3,8] in this work the hybridization of the doping orbitals with the host states is reported. Our study focuses in anatase and rutile TiO_2 doped with Eu ions. In this study density functional theory (DFT) models have been used, and generalized gradient approximation (GGA) and density functional correlated (LDA+U) calculations are presented. In a comparison to experimental data it was found that the GGA calculations show better agreement than LDA+U calculations.

The present work is organized as follows: Sec. II describes the strategy used in the calculations. Section III shows calculated density of states (DOS) per unit cell for TiO_2, and it shows that calculations reproduce well-known electronic properties of anatase (Sec. III A) and rutile (Sec. III B) TiO_2. Section III C presents calculation of effects on the electronic properties of anatase TiO_2 doped with Eu ions. Section III D presents the effects on the electronic properties of rutile TiO_2 doped with Eu ions. Section IV presents our conclusions.

II. METHOD

In our calculations we have used the full-potential linearized augmented plane-wave method (FP-LAPW) as it is implemented in the WIEN2K code.[14] In this method wave functions, charge density, and potential are expanded in spherical harmonics within nonoverlapping muffin-tin spheres, and plane waves are used in the remaining interstitial region of the unit cell. In the code the core and valence states are treated differently. Core states are treated within a multiconfiguration relativistic Dirac-Fock approach, while valence states are treated in a scalar relativistic approach. The exchange-correlation energy was calculated using the GGA correction of Perdew *et al.*[15] Very carefully step analysis is done to ensure convergence of the total energy in terms of the variational cutoff-energy parameter. At the same time

TABLE I. Calculated parameters for anatase TiO_2, compared to experimental data, reported for 15 K, and calculations by other authors.

	Experiment (15 K)[a]	This work	Other work
a (Å)	3.78216(3)	3.83800	3.692[b], 3.784[c]
c (Å)	9.50226(12)	9.64249	9.471[b], 9.515[c]
d^{basal} (Å) 4×	1.9322(11)	1.9589	1.893[b], 1.937[c]
d^{apical} (Å) 2×	1.9788(4)	2.0169	1.948[b], 1.965[c]
u	0.20824(4)	0.20917	0.206[b]
B_o		199.6355	272.11[b]

[a]Reference 18.
[b]Reference 19.
[c]Reference 20.

we have used an appropriate set of k points to compute the total energy. The atomic electronic configuration used in our calculations was O: He $2s^2 2p^4$; Ti: Ar $3d^2 4p^2$; and Eu: Xe $6s^2\ 5d^1\ 4f^6$, and the Eu $5s$ and $5p$ states were treated as valence-band states using local orbital extension of the LAPW method.[14]

Then by computing the total energy of a primitive cell as function of the volume and fitting the data with the Murnaghan[16] equation, the lattice parameters, bulk moduli, and pressure derivative of the bulk module are obtained for anatase and rutile TiO_2. The total energy was minimized for anatase TiO_2 using a set of 99 k points in the irreducible sector of Brillouin zone, equivalent to a $10\times10\times10$ Monkhorst-Pack[17] grid in the unit cell, and a value of 10 Ry for the cutoff energy was used. While for rutile TiO_2 a set of 24 k points, equivalent to a $5\times5\times7$ Monkhorst-Pack[17] grid in the unit cell, and the value of 10 Ry for the cutoff energy were used.

The anatase structure is tetragonal (space group I41/amd) with Ti atoms located at $(0,1/4,3/8)$ and $(0,3/4,5/8)$ and O atoms located at $(0,1/4,z)$, $(0,1/4,1-z)$, $(0,1/4,1/4-z)$, and $(0,1/4,z-1/4)$, and containing 12 atoms in the unit cell. The anatase structure has a TiO_6 octahedron slightly distorted with two apical bond lengths greater than the other four basal bond lengths. For the internal coordinate z, optimized in the calculations, the value $z^{cal}=0.16583$ was obtained, which compares very well with the measured value $z^{exp}=0.16675$.[18] Following Asahi's *et al.*[19] definition for the internal parameter $u=d_{ap}/c$, where d_{ap} is the apical bond length, the calculated value shows better agreement with the experimental value than the calculated by Asahi *et al.*[19] Table I shows that, in general, the calculated structural parameters for anatase TiO_2 are in better agreement than previous published data.[18–20]

The rutile TiO_2 structure is tetragonal with a basis consisting of Ti atoms located at (0,0,0) and $(1/2,1/2,1/2)$, and O atoms located at $(1\pm u,1\pm u,0)$ and $(1/2\pm u,1/2\pm u,1/2)$, with six atoms in the unit cell and a typical value of 0.305 for the internal parameter u. The space group for the structure is P42/mnm. In this structure each Ti atom is coordinate to six O atoms, and each O atom is coordinate to three Ti atoms. It is found that there are two different Ti-O bond lengths, with two Ti-O bonds slightly greater than the other four, the apical and basal bond lengths, respectively. Table II shows our calculated structural parameters and compares them with previous published data.[18,20–22] The table shows that the calculated values are in agreement with the published data.

TABLE II. Calculated parameters for rutile TiO_2, and other reported calculations, compared with experimental data for 15 K.

	Experiment (15 K)[a]	This work	Other work
a (Å)	4.58666(4)	4.60190	4.5936,[b] 4.593[c]
c (Å)	2.955407(3)	2.977400	2.9587[b]
d^{basal} (Å) 4×	1.9459(3)	2.0247	1.949[b], 1.948[c]
d^{apical} (Å) 2×	1.9764(4)	2.0547	1.980[b], 1.982[c]
u	0.30469(6)	0.30392	0.3043[b], 0.305[c]
B_o	216.00[d]	232.02	209.34[b]
B_o'	6.76[d]	6.51	6.11[b]

[a]Reference 18.
[b]Reference 20.
[c]Reference 21.
[d]Reference 22.

Eu impurities have been studied by performing supercell calculations, and the internal atomic coordinates calculated for the pure phases, shown in Tables I and II, have been used as our initial coordinates. Here substitutional defects are considered. The supercell is constituted by multiples of the lattice vectors **a**, **b**, **c**, like the $2\times2\times1$ supercell for the anatase phase, and one Eu ion in a Ti site was substituted. In a similar way, we proceed for the rutile phase, where a $2\times2\times2$ supercell was used. With these constructions a substitution of $Ti_{15}O_{32}Eu_1$ for both the anatase and rutile phases of TiO_2 was done. Then, in order to get the minimum of the total energy for the system, a fully relaxed calculation for all the atomic positions in the supercell was done, where the criterion for convergence was 0.0005 Ry/a.u. The final nearest-neighbor (nn) distances found, between the host atoms and impurities, where slightly different than the calculated for the pure phases. For anatase $Ti_{15}O_{32}Eu_1$ the relaxed nn distances to impurities change from calculated values in pure anatase (shown in Table I) to the next values: basal distances are 2.02142 Å, and the apical distances are 2.04217 Å, values that are 3% bigger than the calculated values in pure anatase. For rutile $Ti_{15}O_{32}Eu_1$, the relaxed nn distances: basal distances are 2.03284 Å, and apical distances are 2.02353 Å, where the apical distances are slightly smaller than that calculated in pure rutile TiO_2 (see Table II).

III. RESULTS AND DISCUSSION

A. Anatase

Figure 1 shows calculated DOS for anatase TiO_2. In the said figure, the zero energy represents the Fermi level. As it is known[20,21,23] the total DOS character in the lower conduction band (CB) has mainly the contribution of the titanium $3d$ states, while the valence-band (VB) states present has the oxygen $2s$- and $2p$-states character. From the figure three groups of bands can be observed; low-lying states around 16

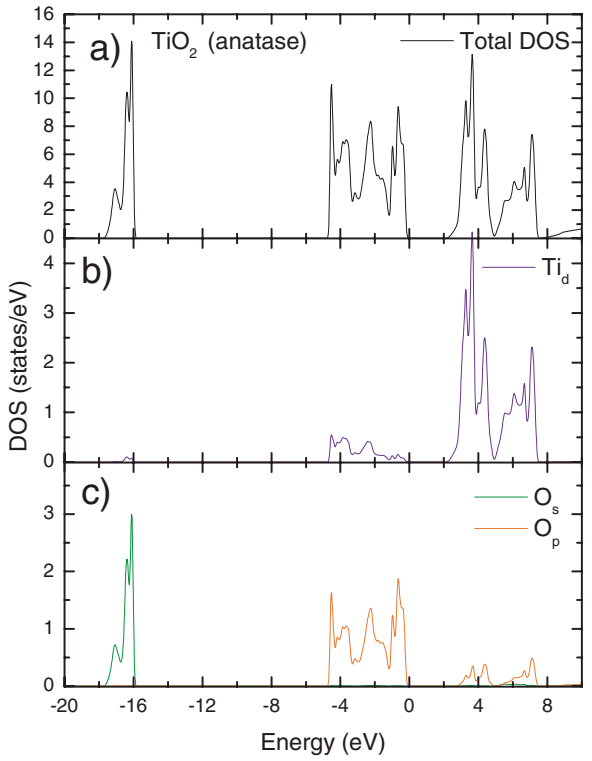

FIG. 1. (Color online) Anatase TiO_2 calculated DOS. Panel (a) total DOS, panel (b) PDOS of Ti 3*d* orbitals (blue line), panel (c) shows O 2*s* (green line) and 2*p* orbitals (red line) PDOS.

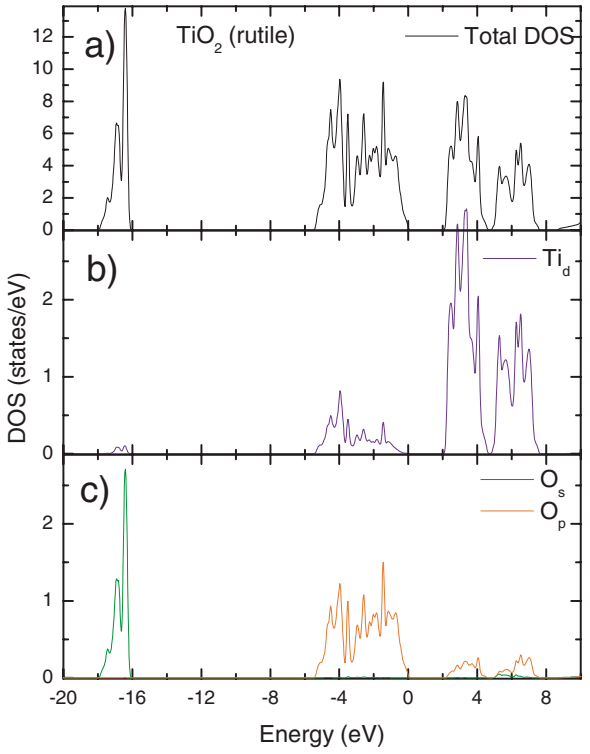

FIG. 2. (Color online) Calculated DOS for rutile TiO_2. Panel (a) total DOS, panel (b) PDOS of Ti 3*d* orbitals (blue line), and panel (c) PDOS of the O 2*s* (green line) and 2*p* orbitals (red line).

eV are coming from the O 2*s* orbitals [green line in Fig. 1(c)], the states just below the Fermi level are coming mainly from the O 2*p* orbitals (red line in Fig. 1(c), and states at energies above the Fermi level have, as the main contribution, the titanium 3*d* character [blue line in Fig. 1(b)]. The calculated bandwidth for the upper VB is 4.76 eV, approximately, which is in agreement with the experimental data (4.75 eV), and shows better agreement than previous calculations.[19,20] The lower VB has a bandwidth of 1.98 eV, approximately, and the main peak is located 16.09 eV below the Fermi level. On the other hand, from our calculations a nonzero titanium partial density of states (PDOS) contribution to the VB states was found. This effect shows the strong hybridization of titanium and oxygen states for these energies. The same is valid for the CB and the hybridization of the oxygen states with the titanium states [see Figs. 1(b) and 1(c)].

B. Rutile

Figure 2 shows calculated DOS for rutile TiO_2. As in the anatase case, the CB states are coming mainly from the Ti 3*d* orbitals [blue line in Fig. 2(b)], while for energies near the top of the VB the O 2*p* orbitals [red line in Fig. 2(c)] have important contributions to these energies, and in the bottom of the VB one band is present, which has the O 2*s*-orbitals character [green line in Fig. 2(c)]. As it was found in calculations, the lower VB bandwidth is 1.98 eV, and the main peak is located at −16.5 eV, while the upper states have a bandwidth of 5.38 eV, approximately. These values are in good agreement with early experimental data (namely, 1.9 eV for the lower band, and 5.4 eV for the upper band,[20] respectively). Similar to the anatase case, from none zero Ti PDOS in the VB region, the hybridization of the titanium and oxygen states in the VB and the hybridization of the oxygen states with the titanium ones in the CB region were obtained.

C. Rare earth impurities in anatase TiO_2: $Ti_{15}O_{32}Eu_1$

Calculated DOS for the system anatase $Ti_{15}O_{32}Eu_1$ are shown in Fig. 3, where for reference the measured band-gap value for pure anatase TiO_2 with vertical lines are represented and the calculated DOS for pure TiO_2 (bold broken line) are also depicted. The main features obtained for pure anatase TiO_2 are also obtained for $Ti_{15}O_{32}Eu_1$. As in pure anatase TiO_2, the main contribution to the total DOS in the upper VB region comes from O 2*p* orbitals, while the lower CB region has mainly Ti 3*d* character. The already commented hybridization of the titanium and oxygen states is also presented in this system. On the other hand, a new series of states in the calculated band gap, as well as in the CB, and in the low VB region besides the well known bands, were obtained. From now on in this work, and as a convention, we will refer to these states as induced states. The obtained differences between the calculated DOS for anatase TiO_2 and $Ti_{15}O_{32}Eu_1$ will be discussed in what follows of the section.

1. Band-gap-induced states

The main contribution to the band-gap-induced states comes from the Eu 4*f* orbitals. To show it in detail, calcu-

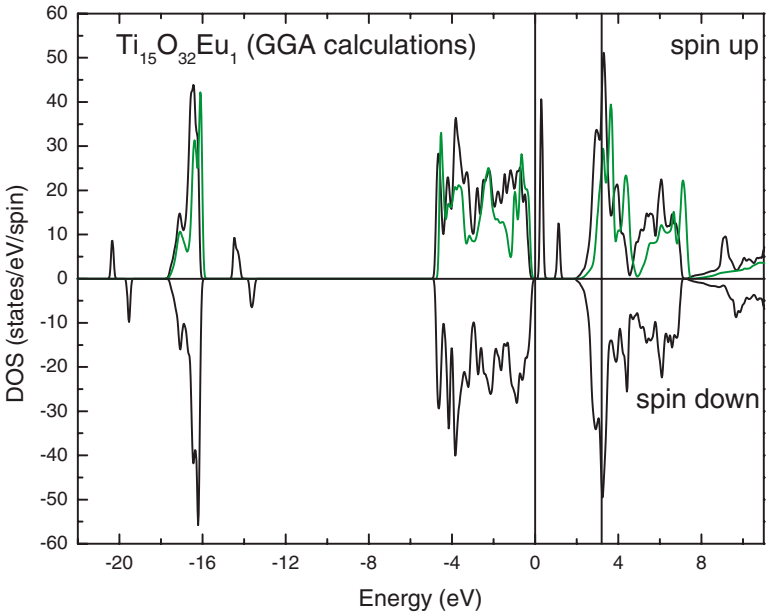

FIG. 3. (Color online) Calculated DOS for anatase $Ti_{15}O_{32}Eu_1$, spin up in the upper side of figure, and spin-down channel in the lower side. Pure anatase TiO_2 DOS is also shown (green bold broken line).

lated 4*f* orbitals are plotted in Fig. 4 and, to complete our discussion, the contribution of the oxygen and titanium states, at these energies, are shown. Figure 4(a) shows the spin-up channel, and Fig. 4(b) shows the spin-down channel. The spin-up-induced states are located just above the maximum of the VB [Fig. 4(a)], while the spin-down-induced states are located near the minimum of the CB [Fig. 4(b)]. Figure 4(a) shows that the spin-up-induced states have an important contribution from the O 2*p* orbitals and Ti 3*d* orbitals. This effect manifests the hybridization of the local orbitals with the Eu 4*f* orbitals. Similar effects have been observed for systems such as $Ga_{1-x}Cr_xN$. Cr ions induce electronic states in the band gap of GaN, and it is interpreted that Cr 3*d* orbitals hybridize with Ga 4*s* orbitals.[24] The same is also reported for other diluted magnetic semiconductors, where *d* impurity levels hybridize with local VB *p* states.[25]

On the other hand, from experimental point of view it is reported that after doping TiO_2 with Eu, a red emission is obtained.[4–7] This emission is associated with an Eu intra-4*f* transition. In order to reproduce the experimental values (namely 2.014–2.018 eV) in the present calculations, a transition from the spin-down states to the spin-up states should be obtained, and these states should be pinned in the band gap of the compound. To get this condition, and reproduce the experimental band gap of anatase TiO_2 [3.2 eV (Ref. 20)] rigidly, the minimum of the CB have to be moved. This procedure is accepted as valid if the exciting properties from the host matrix are not disturbed.[26] Figure 4 shows the effect of applying the scissors operator to the lowest CB states to adjust the experimental band gap (vertical lines). Then, after

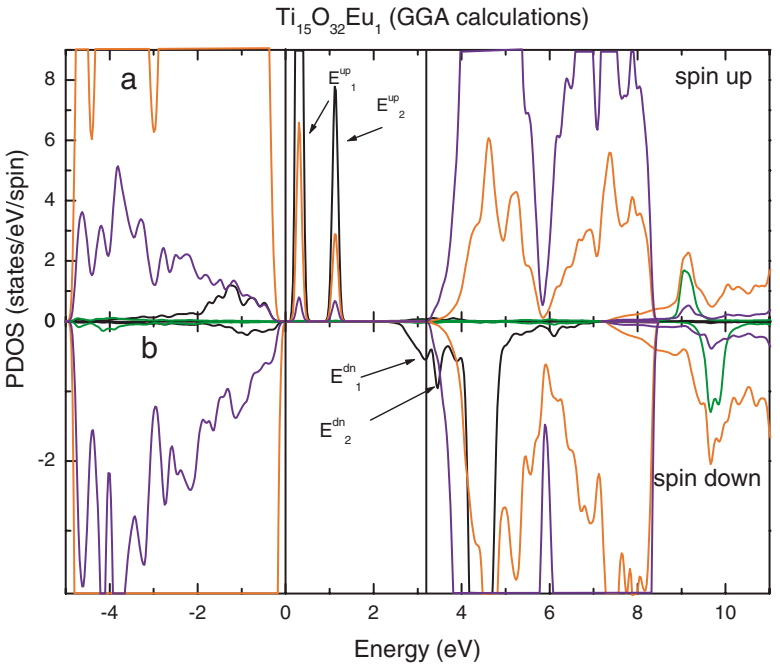

FIG. 4. (Color online) Calculated PDOS for anatase $Ti_{15}O_{32}Eu_1$. Eu 4*f* (black line), 5*d* orbitals (green line), O 2*p* (red line), and Ti 3*d* orbitals (blue line). Spin-up channel upper panel, while spin down shown in the lower panel.

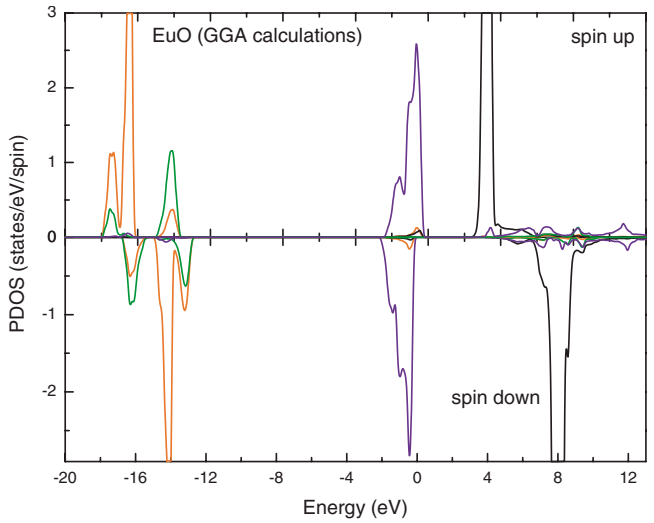

FIG. 5. (Color online) Lanthanide EuO calculated PDOS. Eu 4*f* (black line), 5*p* orbitals (red line), O 2*s* (green line) and 2*p* orbitals (blue line). Spin-up channel in the upper side and the spin-down channel in the lower side.

the O and Ti states from minimum of the CB was moved, keeping fix the Eu states, a set of Eu intra-4*f* transitions in the interval of energies from 2.05→4.21 eV are obtained, values that are in the red emission experimental range for the $Ti_{15}O_{32}Eu_1$ (Refs. 4–7) system. In Fig. 4 the transitions from the peaks labeled E^1_{dn} and E^2_{dn} to E^2_{up} give the values 2.05 and 2.07 eV, respectively. Thus, the calculations reproduce the observed red emission in $Ti_{15}O_{32}Eu_1$.

2. Induced states and the CB

Then, in the high-energy region, at 9.09 eV for the spin-up channel and at 9.63 eV for the spin-down channel, Figs. 3 and 4 show a set of bands with a great contribution from the Eu 5*d* orbitals. However, an important contribution of O 2*p* orbitals and Ti 3*d* orbitals to these bands was also found.

3. Induced states and the VB

Finally, at low energies in the VB region, Fig. 3 shows an interesting effect over the deeper band, the originally O 2*s* band—we obtained a band folding. The main peak of these set of bands is located at −16.44 eV for the spin-up channel, and at −16.22 eV for the spin-down channel, slightly lower than in pure anatase TiO_2 (namely, −16.09 eV). As it should be expected the main contribution to this band comes from the O 2*s* orbitals. The other bands are located at 14.48 and 20.35 eV for the spin-up channel, and 13.63 and 19.54 eV for the spin-down channel, below Fermi level, respectively. The additional bands are a hybridization of the Eu $5p^{\uparrow\downarrow}$ orbitals with the O 2*s* and 2*p* orbitals.

A similar hybridization of RE 5*p* orbitals with O 2*s* and 2*p* orbitals in the lanthanide oxides are reported.[27–32] The electronic band structure of the lanthanide oxide EuO (Ref. 33) was calculated to show that this effect is the origin of folding of the O 2*s* band. Figure 5 shows calculated PDOS for EuO, where the Eu 4*f* and 5*p* orbitals, and the O 2*s* and 2*p* orbitals are depicted. From the figure, in the low VB region, the interaction between the Eu 5*p* orbitals and the O 2*s* and 2*p* orbitals gives origin to a three-band set. In cubic EuO the main contribution to these bands comes from the Eu 5*p* orbitals, while in tetragonal $Ti_{15}O_{32}Eu_1$ the main contribution to these bands comes from O 2*s* character. However, the additional bands are the hybridization of the Eu 5*p* and O 2*s* orbitals. From these facts, we conclude that the pattern obtained for the low VB range in tetragonal $Ti_{15}O_{32}Eu_1$ is similar to that obtained in cubic EuO, showing in this way the hybridization of Eu orbitals with the tetragonal TiO_2 orbitals at these energies. Then, for energies near the Fermi level, the upper VBs are mainly O 2*p* in character. While the Eu 4*f* orbitals are located above the Fermi level. The spin–up bands are located at 3.29 eV and spin down bands are located at 8.05 eV, in agreement with early reports.[27–31]

4. LDA+U calculations

It is worthy to note that in recent works, it is discussed that in order to locate properly the RE 4*f* states, it is necessary to use density-functional-correlated band-theory calculations (LDA+U calculations).[34–38]

To verify the influence of these corrections on the electronic properties of the systems, LDA+U calculations for tetragonal $Ti_{15}O_{32}Eu_1$, as well as for cubic EuO, were done. In these calculations it is known that a great value for the onsite Coulomb interaction U parameter is necessary, as well as that different values used for U_f in europium compounds range from 7 to 10 eV.[34,39,40] At the same time, recently, Steeneken *et al.*[34] show that in EuO, the U_f=7.0 eV value reproduce properly the experimental data. The same value has been used by other authors to study europium chalcogenides and pnictides,[36] showing good results. Then assuming that this is a reasonable value for U_f, the value U_f =7.0 eV was used in the present study (although more work it is necessary in order to find appropriate values for the interaction parameter[41]).

As it is obtained in our calculations, the Eu 4*f* spin-up states are energy shifted downward, while the Eu 4*f* spin-down states are shifted upward. In the EuO case the states are shifted 3 eV, approximately, downward and upward, respectively. In such a way, the spin-up states are almost at the Fermi level, and the spin-down states are at higher energies in the CB region, and their energy difference is approximately 11 eV. Similar results are obtained for tetragonal $Ti_{15}O_{32}Eu_1$. A splitting for the Eu 4*f* spin-up states is obtained; now they are near the Fermi level, as well as in the low CB region (the main peaks are located at –0.02, 2.85, and 3.74 eV, respectively), while the 4*f* spin-down states are at higher energies in the CB (the two main peaks are located at 6.08 and 6.92 eV). In order to show these results, the calculated PDOS for this system is depicted in Fig. 6. From these results, the Eu 4*f* transitions discussed above, the transitions for the spin-down states to the band-gap spin-up states, are not allowed in this case. At the same time, for the Eu 4*f* spin-up band located in the band gap, the hybridization of this band with the O 2*p* and Ti 3*d* states is obtained, as in

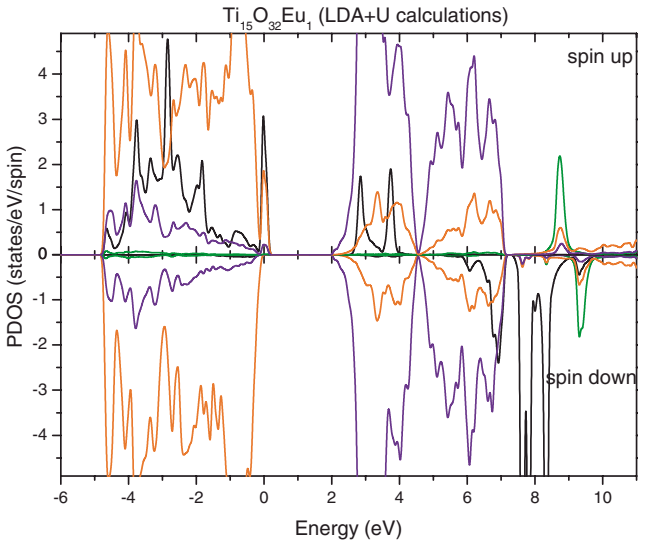

FIG. 6. (Color online) Calculated PDOS for anatase $Ti_{15}O_{32}Eu_1$, using LDA+U corrections. Value used for U_f=7 eV (Ref. 34). Eu 4*f* (black line), 5*d* orbitals (green line), O 2*p* (red line), and Ti 3*d* orbitals (blue line). Spin-up channel in upper panel, while the spin down in the lower panel.

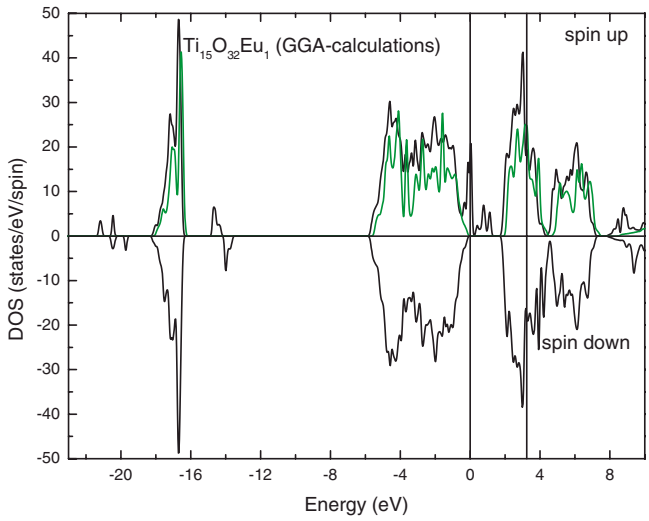

FIG. 7. (Color online) Calculated DOS for rutile $Ti_{15}O_{32}Eu_1$, and for comparison the calculated DOS for pure rutile TiO_2 are shown (green broken line).

the GGA calculations. The Eu 5*d* states (green lines) are obtained at the same energies in the CB as were obtained in GGA calculations. This should be the case because the LDA+U corrections were not applied to these states.

On the other hand, different authors[42–44] show that in most RE metals, DFT calculations in the GGA approximation, including spin polarization, describe properly the strong Coulomb correction, and it is believed that this is because GGA treats the nonlocality of exchange-correlation better than LDA.

According to these comments and from our results we observe that using LDA+U corrections in our study of TiO_2 doped with RE ions, the Eu intra-4*f* transitions are not obtained. Similar results have been obtained for rutile $Ti_{15}O_{32}Eu_1$, as will be shown in next section.

D. Rare earth impurities in rutile TiO_2: $Ti_{15}O_{32}Eu_1$

Figure 7 shows calculated DOS for rutile $Ti_{15}O_{32}Eu_1$. As in previous case, for comparison, calculated DOS for the pure rutile TiO_2 are plotted.

In general, the calculated DOS for rutile $Ti_{15}O_{32}Eu_1$ are obtained and have almost the same characteristics calculated for pure rutile TiO_2. As in the anatase case, the induced states are obtained the same in the VB, as well as in the CB region.

1. Band-gap-induced states

The band-gap induced-states have mainly the Eu 4*f* character, with a small contribution from the O 2*p* and Ti 3*d* orbitals. The induced states for the spin-up channel show three well-localized bands, and the spin-down induced-states are inside the low CB states. Moving rigidly the minimum of the CB states, applying the scissors operator to the lowest CB states, in order to obtain the experimental band-gap value of rutile TiO_2 [3.24 eV (Ref. 20)], we have that the lower spin-down-induced states are located at 3.92 eV (see Fig. 8 for details). Transitions from these bands to the spin-up states will be in the next energy range: 2.80, 3.16, and 3.54 eV (in Fig. 8: transitions from the peak labeled E^1_{dn} to peaks E^1_{up}, E^2_{up}, E^3_{up}, respectively), the values are in the range reported for Eu in the lamellar titania nanoshets.[7] Assuming that the Eu intra-4*f* transition is allowed, i.e., that there are no transitions from the Eu 4*f* spin-down states to the local Ti 4*d* states or O 2*p* states, then our calculations reproduce the experimental data for the red emission in rutile $Ti_{15}O_{32}Eu_1$.

2. Induced states and the CB

In the CB, at high energies, the Eu 5*d* band is obtained. For the spin-up channel this band is located at 8.79 eV, and for the spin-down channel, this band is located at 9.38 eV. As in previous case, these bands hybridize with the O 2*p* and Ti 3*d* orbitals.

3. Induced states and the VB

Finally, in the low VB region, Fig. 7 shows that the initially O 2*s* band is folded in four bands. While in the anatase:Eu case, three bands were obtained for this energy region (following the pattern showed by cubic EuO); here we obtain four bands. The main peak for these set of bands has the O 2*s* character, as it is obtained for pure rutile, and it is located at −16.71 eV for both the spin-up and spin-down channel (while in pure rutile TiO_2 the peak is located at −16.5 eV). The other three bands are a hybridization of the O 2*s* and 2*p* orbitals with the Eu 5*p* orbitals. For the spin-up channel these bands are located at −14.67, −20.46, and −21.17 eV, while for the spin down channel they are located at −13.99, −19.73, and −20.46 eV, respectively.

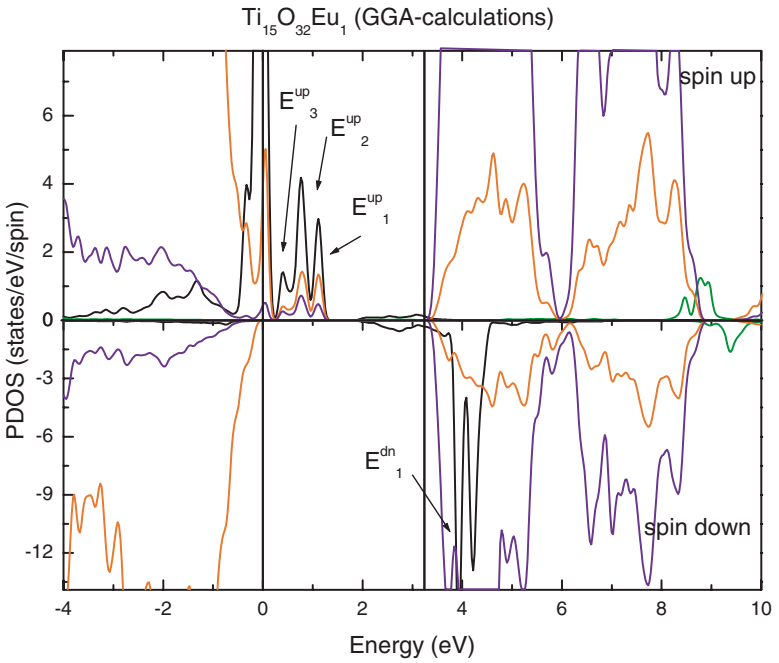

FIG. 8. (Color online) Calculated PDOS for rutile $Ti_{15}O_{32}Eu_1$. Eu $4f$ (black line), $5d$ orbitals (green line), O $2p$ (red line), and Ti $3d$ orbitals (blue line). Spin-up channel, the upper panel, while spin down in the lower panel.

4. LDA+U calculations

Figure 9 shows LDA+U calculations for rutile $Ti_{15}O_{32}Eu_1$. As in previous case, the value U_f=7.0 eV was used for the onsite Coulomb interaction parameter, assuming that this is a good value for U_f. Two spin-up-induced states well localized in the band gap were obtained (notice the hybridization of the O $2p$ and Ti $3d$ states with the induced states, already obtained in the GGA calculations). However, the spin-down-induced states are located at high energies in the CB. This means that the intra-$4f$ transitions that we are looking for in this case would be 4.9 and 5.4 eV for the transition from the lower spin-down state to the spin-up induced states located in the band gap. These values are bigger than experimental data. As we have noticed above, similar results were obtained for the anatase:Eu case.

These results corroborate our previous conclusion that for anatase and rutile $Ti_{15}O_{32}Eu_1$ system, GGA calculations are better than LDA+U calculations.

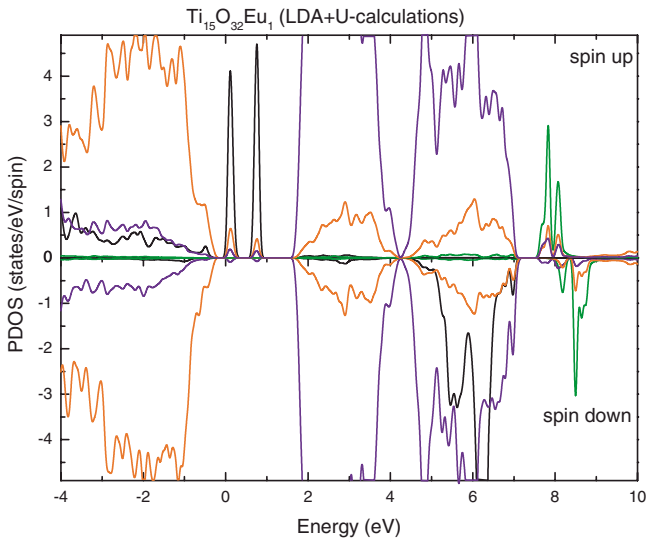

FIG. 9. (Color online) Rutile $Ti_{15}O_{32}Eu_1$ calculated PDOS, using LDA+U corrections. U_f=7 eV (Ref. 34). Eu $4f$ (black line), $5d$ orbitals (green line), O $2p$ (red line), and Ti $3d$ orbitals (blue line). Spin-up channel in upper panel, spin down, lower panel.

E. Last remarks

A final comment related with the induced states obtained doping TiO_2 with other RE ions is addressed here: GGA calculations for anatase and rutile TiO_2 doped with Gd and Tb ions were done. As we found, the spin-up-induced states are in resonance with the host VB states, while the spin-down-induced states are located in the low CB region in such a way that our calculated values for RE intra-$4f$ transitions are not in agreement with experimental reports (details will be published elsewhere). However, the hybridization shown for the Eu induced states with the host VB and CB states is also obtained by doping TiO_2 with Gd and Tb ions. It is interesting to note that the band-gap-induced states move downward in energy as the atomic number of the RE ion increases. Also worth noting is the well-resolved sharp obtained for the induced states in anatase TiO_2 in comparison to the rutile phase. This last result, support previous experimental facts that doping TiO_2 with RE ions favors anatase phase.[12]

IV. CONCLUSIONS

Ab initio study of the effects on the electronic properties of anatase and rutile TiO_2 doped with Eu ions was done with very good results. Although some authors suggest to use LDA+U calculations to study the RE $4f$ states, here we found that GGA calculations reproduce quite properly experimental values for $Ti_{15}O_{32}Eu_1$ in both anatase and rutile phase.

The introduction of Eu ions in the matrix TiO_2 has as a consequence that besides the states induced in the band gap, an important interaction between the host VB and CB states and the Eu orbitals is also obtained.

Contrary to the widely accepted idea that RE orbitals should be pinned in the band gap as atom-free-like states, our results show that although in a first approach, the band-gap-induced states can be treated as highly localized; these states have a non-negligible hybridization with the local O 2*p* and Ti 3*d* states.

For the high CB energies, one band mixing Eu 5*d* orbitals with the O 2*p* and Ti 3*d* orbitals was obtained.

For the lower VB states, the initially O 2*s* band is splitted due to the interaction of the Eu 5*p* orbitals with the O 2*s* and 2*p* orbitals. This interaction is similar to the effect obtained in lanthanide oxides.

ACKNOWLEDGMENTS

This work was done using the Computer Facilities of IPICYT, San Luis Potosí, México. The authors are indebted to E. G. Poulain-García and A. Rodríguez–Soria for a critical reading of the manuscript. This work was completed while DO was in a research stay at Freie Universität Berlin, the hospitality of H. Kleinert is greatly appreciated. DO gratefully acknowledges financial support from CINVESTAV-IPN and CONACYT-México.

[1] R. Janisch and N. A. Spaldin, Phys. Rev. B **73**, 035201 (2006).
[2] T. Chanier, M. Sargolzaei, I. Opahle, R. Hayn, and K. Koepernik, Phys. Rev. B **73**, 134418 (2006).
[3] K. L. Frindell, M. H. Bartl, M. R. Robinson, G. C. Bazan, A. Popitsch, and G. D. Stucky, J. Solid State Chem. **172**, 81 (2003), and references therein.
[4] A. Conde-Gallardo, M. García Rocha, and I. Hernández-Calderón, Appl. Phys. Lett. **78**, 3436 (2001).
[5] M. García Rocha, A. Conde-Gallardo, I. Hernández-Calderón, and R. Palomino-Merino, Mod. Phys. Lett. B **15**, 769 (2001).
[6] A. Conde-Gallardo, M. García Rocha, I. Hernández-Calderón, and R. Palomino-Merino, Mod. Phys. Lett. B **15**, 813 (2001).
[7] H. Xin, R. Ma, L. Wang, Y. Ebina, K. Takada, and T. Sasaki, Appl. Phys. Lett. **85**, 4187 (2004).
[8] C. Delerue and M. Lannoo, Phys. Rev. Lett. **67**, 3006 (1991).
[9] A.-W. Xu, Y. Gao, and H.-Q. Liu, J. Catal. **207**, 151 (2002).
[10] C. Mignotte, Appl. Surf. Sci. **226**, 355 (2004).
[11] S.-Y. Chen, C.-C. Ting, and W.-F. Hsich, Thin Solid Films **434**, 171 (2003).
[12] S. Jeon and P. W. Braun, Chem. Mater. **15**, 1256 (2003).
[13] H. Amekura, A. Eckau, R. Carius, and Ch. Buchal, J. Appl. Phys. **84**, 3867 (1998).
[14] P. Blaha, K. Schwarz, G. K. H. Madsen, D. Kvasnicka, and J. Luitz, *WIEN2k, An Augmented Plane Wave Plus Local Orbitals Program for Calculating Crystal Properties* (Vienna University of Technology, Austria, 2001).
[15] J. P. Perdew and Y. Wang, Phys. Rev. B **45**, 13244 (1992); J. P. Perdew, K. Burke, and M. Ernzerhof, Phys. Rev. Lett. **77**, 3865 (1996).
[16] F. D. Murnaghan, Proc. Natl. Acad. Sci. U.S.A. **30**, 244 (1944).
[17] H. J. Monkhorst and J. D. Pack, Phys. Rev. B **13**, 5188 (1976).
[18] J. K. Burdett, T. Hughbanks, G. J. Miller, J. W. Richardson, and J. V. Smith, J. Am. Chem. Soc. **109**, 3639 (1987).
[19] R. Asahi, Y. Taga, W. Mannstadt, and A. J. Freeman, Phys. Rev. B **61**, 7459 (2000).
[20] S.-D. Mo and W. Y. Ching, Phys. Rev. B **51**, 13023 (1995).
[21] P. I. Sorantin and K. Schwarz, Inorg. Chem. **31**, 567 (1992).
[22] M. H. Manghnani, J. Geophys. Res. **74**, 4317 (1969); M. H. Manghnani, E. S. Fisher, and W. S. Brower, Jr., J. Phys. Chem. Solids **33**, 2149 (1972).
[23] M. A. Khan, A. Kotani, and J. C. Parlebas, J. Phys.: Condens. Matter **3**, 1763 (1991).
[24] J. J. Kim, H. Makino, K. Kobayashi, Y. Takata, T. Yamamoto, T. Hanada, M. W. Cho, E. Ikenaga, M. Yabashi, D. Miwa, Y. Nishino, K. Tamasaku, T. Ishikawa, S. Shin, and T. Yao, Phys. Rev. B **70**, 161315(R) (2004).
[25] K. Sato and H. Katayama-Yoshida, Jpn. J. Appl. Phys., Part 2 **40**, L485 (2001).
[26] Due to the band-gap problem in *ab initio* calculations and to reproduce optical properties, it is widely accepted to move rigidly the minimum of the conduction band using the so-called scissors operator, assuming exciting properties of the compound are not disturbed, see, for example, G. A. Baraff and M. Schlüter, Phys. Rev. B **30**, 3460 (1984); M. R. Pederson and B. M. Klein, *ibid.* **37**, 10319 (1988); F. Gygi and A. Baldereschi, Phys. Rev. Lett. **62**, 2160 (1989); N. E. Christensen, in *High Pressure in Semiconductor Physics*, edited by T. Suski and W. Paul, Vol. 54of Semiconductors and Semimetals (Academic, New York, 1998), p. 49, and references therein.
[27] S. G. Wang, D. K. Pan, and W. H. E. Schwarz, J. Chem. Phys. **102**, 9296 (1995).
[28] E. Byrom, D. E. Ellis, and A. J. Freeman, Phys. Rev. B **14**, 3558 (1976).
[29] S. J. Cho, Phys. Rev. B **1**, 4589 (1970).
[30] D. E. Eastman, F. Holtzberg, and S. Methfessel, Phys. Rev. Lett. **23**, 226 (1969).
[31] P. M. Grant and J. C. Suits, Appl. Phys. Lett. **14**, 172 (1969).
[32] Effect also obtained in the rare-earth pnitides like GdN, F. Leuenberger, A. Parge, W. Felsch, K. Fauth, and M. Hessler, Phys. Rev. B **72**, 014427 (2005).
[33] EuO crystallizes in a fcc NaCl-type cell space group $Fm\bar{3}m$, with lattice parameter $a=5.141$ Å, B. T. Matthias, R. M. Bozorth, and J. H. Van Vleck, Phys. Rev. Lett. **7**, 160 (1961).
[34] P. G. Steeneken, L. H. Tjeng, I. Elfimov, G. A. Sawatzky, G. Ghiringhelli, N. B. Brookes, and D.-J. Huang, Phys. Rev. Lett. **88**, 047201 (2002).
[35] J. Kuneš, W. Ku, and W. E. Pickett, J. Phys. Soc. Jpn. **74**, 1408 (2005).
[36] M. Horne, P. Strange, W. M. Temmerman, Z. Szotek, A. Svane, and H. Winter, J. Phys.: Condens. Matter **16**, 5061 (2004).
[37] M. D. Johannes and W. E. Pickett, Phys. Rev. B **72**, 195116 (2005).

[38] P. Novák, J. Kuneš, L. Chaput, and W. E. Picket, Phys. Status Solidi B **243**, 559 (2006).
[39] G. K. H. Madsen, K. Schwarz, P. Blaha, and D. J. Singh, Phys. Rev. B **68**, 125212 (2003).
[40] V. N. Antonov, B. N. Harmon, and A. N. Yaresko, Phys. Rev. B **72**, 085119 (2005).
[41] We have done LDA+U calculations using the value U=7.5 eV, and we obtain that the band-gap spin-up-induced states are located almost 0.02 eV downward in energy, and the spin down states are located 0.10–0.30 eV upward in comparison to the U=7.0 eV calculation. The shape of the hybidrization of the obtained bands are the same as that shown in Fig. 6.
[42] S. J. S. Jalali Asadabadi and H. Akbarzadeh, Physica B (Amsterdam) **349**, 76 (2004).
[43] A. Delin, P. M. Oppeneer, M. S. S. Brooks, T. Kraft, J. M. Wills, B. Johansson, and O. Eriksson, Phys. Rev. B **55**, R10173 (1997).
[44] A. Delin, L. Fast, B. Johansson, O. Eriksson, and J. M. Wills, Phys. Rev. B **58**, 4345 (1998).